

Make Anything Match Your Target: Universal Adversarial Perturbations against Closed-Source MLLMs via Multi-Crop Routed Meta Optimization

Hui Lu¹ Yi Yu¹ Yiming Yang¹ Chenyu Yi¹ Xueyi Ke¹ Qixing Zhang¹ Bingquan Shen² Alex Kot¹
Xudong Jiang¹

Abstract

Targeted adversarial attacks on closed-source multimodal large language models (MLLMs) have been increasingly explored under black-box transfer, yet prior methods are predominantly *sample-specific* and offer limited reusability across inputs. We instead study a more stringent setting, Universal Targeted Transferable Adversarial Attacks (UTTAA), where a single perturbation must consistently steer arbitrary inputs toward a specified target across unknown commercial MLLMs. Naively adapting existing sample-wise attacks to this universal setting faces three core difficulties: (i) target supervision becomes high-variance due to target-crop randomness, (ii) token-wise matching is unreliable because universality suppresses image-specific cues that would otherwise anchor alignment, and (iii) few-source per-target adaptation is highly initialization-sensitive, which can degrade the attainable performance. In this work, we propose MCRMO-Attack, which stabilizes supervision via Multi-Crop Aggregation with an Attention-Guided Crop, improves token-level reliability through alignability-gated Token Routing, and meta-learns a cross-target perturbation prior that yields stronger per-target solutions. Across commercial MLLMs, we boost unseen-image attack success rate by +23.7% on GPT-4o and +19.9% on Gemini-2.0 over the strongest universal baseline.

1. Introduction

Building upon the significant advancements in Large Language Models (LLMs) (Touvron et al., 2023; Bai et al., 2023a), Multi-modal Large Language Models (MLLMs) have recently attracted substantial attention (Zhu et al., 2023a; Lu et al., 2024; Li et al., 2025a). However, despite their potential, the safety of MLLMs remains a critical chal-

lenge, as existing models have been shown to be susceptible to adversarial attacks (Jiang et al., 2025). In particular, targeted adversarial attacks are of special concern, as they aim to deliberately induce specific, attacker-chosen incorrect outputs, in contrast to untargeted attacks that cause arbitrary prediction failures (Zhao et al., 2023; Guo et al., 2024).

Commercial closed-source MLLMs, *e.g.*, GPT-4o (Achiam et al., 2023), Claude-4.5 (Anthropic, 2025), and Gemini-2.0 (Team et al., 2023), are not immune to such vulnerabilities. In practice, attackers can exploit the transferability of adversarial perturbations crafted on accessible surrogate models to mount black-box attacks against proprietary systems (Lu et al., 2026; Li et al., 2025b). Furthermore, perturbations optimized on open-source CLIP models have been shown to induce targeted mispredictions on closed-source MLLMs. Nevertheless, the efficacy of these transfer-based targeted adversarial attacks is often hampered by limited generalization to unseen images. Prior approaches employ a sample-wise optimization strategy (Jia et al., 2025; Li et al., 2025b), in which instance-specific perturbations are independently tailored to each input. While effective on source images, such perturbations tend to overfit to local visual patterns or specific semantic cues, failing to retain adversarial potency when applied to different images, as shown in Fig. 1. This undermines the practical utility of targeted adversarial attacks, as optimizing unique perturbations for each input is computationally prohibitive or impractical in real-world settings. Consequently, we are motivated to explore an effective universal and transferable targeted-attack method with strong generalization across diverse visual inputs.

A straightforward approach is to extend existing sample-wise methods to the universal setting; however, this strategy can be brittle for two key reasons. First, the combination of a source image pool and crop-based alignment introduces triple randomization, including random source selection and independent cropping of both source and target, which hinders stable optimization. Second, the lack of explicit guidance over token alignment forces the optimizer to implicitly decide “what to match”, with many tokens corresponding to background, incidental patterns, or crop-induced noise. Forcing such weakly aligned tokens to match the target introduces spurious supervision and misguides the optimization.

In light of this, we propose **MCRMO-Attack**, which aims

¹Nanyang Technological University ²DSO National Laboratories. Correspondence to: Yi Yu <yu.yi@ntu.edu.sg>.

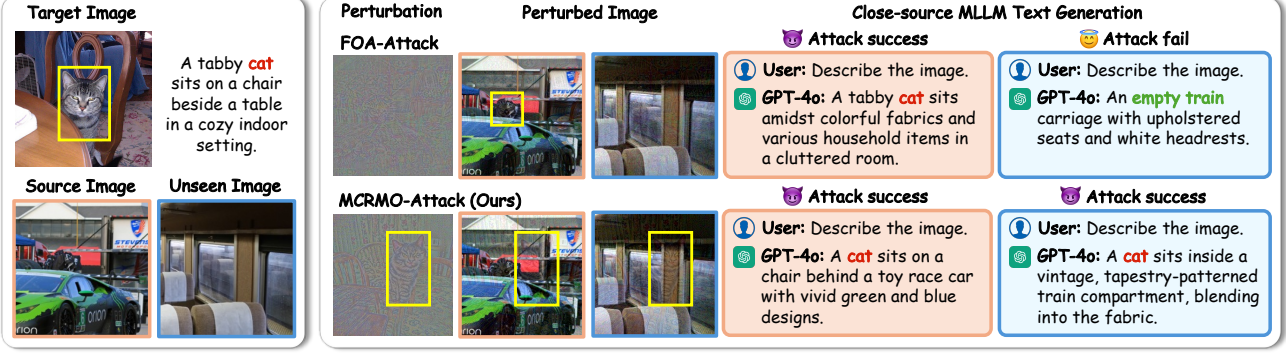


Figure 1. Comparison of targeted adversarial examples generated by FOA-Attack (Jia et al., 2025) and our MCRMO-Attack on the source image (captions in orange box) and an unseen arbitrary image (captions in blue box). Both methods succeed on the source images. However, FOA-Attack relies on local shadow cues and fails to transfer, while our MCRMO-Attack consistently induces the target concept (“cat”) across heterogeneous backgrounds. Best viewed via zoom-in.

to craft a universal perturbation capable of misleading closed-source MLLMs toward desired target outputs, independently of individual image characteristics. To stabilize learning, we introduce **Multi-Crop Aggregation (MCA)** with an **Attention-Guided Crop (AGC)**. Instead of relying on a potentially noisy local crop (Jia et al., 2025; Li et al., 2025b), this strategy aggregates supervisory signals across multiple target crops, allowing the optimization to capture more consistent target-specific characteristics. Moreover, we leverage a **Token Routing (TR)** mechanism to explicitly guide the model toward *where* to attend during universal perturbation learning. By selectively emphasizing these alignable tokens, it is able to deliver more stable learning signals. At the same time, non-alignable tokens are regularized to remain close to their original source representations, preventing them from steering the perturbation toward trivial or noisy directions. Furthermore, we adopt a **Meta-Initialization (MI)** scheme that learns a target-agnostic perturbation prior by exposing the optimization process to a wide range of target concepts during meta-training. This initialization captures shared and transferable structures across targets, enabling the learned initial perturbation to generalize effectively to each target. Notably, with meta-initialization, our method achieves attack performance that is comparable to or even surpasses optimization from scratch with substantially more iterations (*e.g.*, 50 steps w/ MI versus 300 steps w/o MI).

Our main contributions are summarized as follows:

- We present the first systematic study of **universal targeted transferable adversarial attacks** against closed-source MLLMs, a substantially more challenging setting than previous sample-wise attacks.
- We propose MCRMO-Attack, a universal targeted transferable adversarial attack that jointly stabilizes universal learning via MCA with AGC, enhances informative su-

pervision through TR with selective alignment, and learns a target-agnostic perturbation prior through MI.

- Extensive experiments demonstrate that adversarial perturbations generated by our MCRMO-Attack exhibit strong generalization to previously unseen images across multiple commercial MLLMs, while remaining competitive with sample-wise methods on seen source images. In particular, our approach improves upon the SOTA universal attacks by an **absolute 23.7%** on GPT-4o and **19.9%** on Gemini-2.0 in attack success rate for unseen images.

2. Related Work

Multi-modal Large Language Models. Recent progress in LLMs (Touvron et al., 2023; Bai et al., 2023a) has spurred growing interest in MLLMs, which integrate language understanding with visual modality (Bai et al., 2023b; Zhu et al., 2023a; Li et al., 2025a). Representative models such as LLaVA (Liu et al., 2023) and DeepSeek-VL (Lu et al., 2024) demonstrate impressive capabilities across a wide range of multimodal tasks, including image captioning (Salaberria et al., 2023), visual question answering (Kuang et al., 2025), and visual complex reasoning (Li et al., 2024). In addition to open-source progress, several commercial closed-source MLLMs, such as GPT-4o (Achiam et al., 2023), Claude-4.5 (Anthropic, 2025), and Gemini-2.0 (Team et al., 2023), have also been widely adopted.

Transferable Adversarial Attack. Transfer-based attacks craft adversarial examples on accessible surrogate models and transfer them to unseen victims. Prior work improves transferability mainly via: (i) optimization refinements for more model-agnostic gradients (FGSM/iterative variants, momentum, smoothing) (Kurakin et al., 2018; Dong et al., 2018; Zhu et al., 2023b); (ii) input diversification with stochastic transforms (resize-pad, multi-scale, translation, mixing, block-wise) (Xie et al., 2019; Lin et al., 2019; Dong

et al., 2019; Wang et al., 2021a; 2024b); and (iii) feature-level manipulation (highlighting influential neurons or aligning intermediate patterns) (Ganeshan et al., 2019; Wang et al., 2021b; Zhang et al., 2022a;b; Liang et al., 2025).

Targeted Attack on MLLMs. Attacks on MLLMs can be untargeted (degrading responses) or targeted (steering outputs to a specified goal). Recent work increasingly studies *transferable targeted* attacks, including surrogate-based transfer (Zhao et al., 2023), diffusion-guided optimization (Guo et al., 2024), and frequency/ensemble-enhanced black-box methods (Dong et al., 2023). Transfer is further boosted by stronger surrogates/generators (Zhang et al., 2025b), lightweight stochastic augmentations (Li et al., 2025b), and joint global-local feature alignment for proprietary models (Jia et al., 2025; Hu et al., 2025).

Our Motivation. While universal transferable attacks on MLLMs have attracted increasing attention in recent years (Zhang et al., 2024; Yang et al., 2024; Zhou et al., 2025b; 2023), we focus on a substantially more challenging *targeted universal* setting, in which a single perturbation must consistently steer model outputs toward a specified target. Unlike X-Transfer (Huang et al., 2025), whose targets are limited to 10 fixed text descriptions, our framework supports arbitrary target images, providing a richer and more realistic target space for vision-centric tasks.

3. Preliminary and Problem Formulation

Existing transfer-based targeted adversarial attacks against closed-source MLLMs typically operate in a *sample-wise* manner (Jia et al., 2025; Li et al., 2025b): they optimize an instance-specific perturbation for each input image \mathbf{x} . While effective for the given sample, the learned perturbation δ typically fails to generalize to unseen images $\mathbf{x}' \neq \mathbf{x}$, requiring computationally expensive re-optimization for every new input \mathbf{x}' . We instead study a **Universal Targeted Transferable Adversarial Attack (UTTAA)**, which learns a *single*, input-agnostic perturbation that, for *arbitrary* inputs, steers the victim MLLM’s output (or visual embedding) toward the target image \mathbf{x}_{tar} . Our objective is formulated as follows:

Definition 3.1 (UTTAA). Given a target image $\mathbf{x}_{\text{tar}} \in \mathbb{R}^{H \times W \times C}$ and a feasible space \mathcal{S} (e.g., $\|\delta\|_{\infty} \leq \frac{16}{255}$), a universal targeted transferable perturbation is a single perturbation δ (shared across inputs) that, when added to an arbitrary clean image, drives unknown victim models to match the target in the specified representation space:

$$\delta^* \in \arg \min_{\delta \in \mathcal{S}} \mathbb{E}_{\underline{\mathbf{x}} \sim \mathcal{D}} \mathbb{E}_{\hat{\mathbf{f}} \sim \hat{\mathcal{F}}} [\mathcal{L}_{\text{eval}}(\mathbf{x} + \delta, \mathbf{x}_{\text{tar}}; \hat{\mathbf{f}})], \quad (1)$$

where \mathbf{x} is an arbitrary clean image sampled from a natural distribution \mathcal{D} , $\hat{\mathcal{F}}$ is a family of (unknown) victim MLLMs, and $\mathcal{L}_{\text{eval}}(\cdot)$ is an external, output-level discrepancy that compares the model response to the perturbed image $\hat{\mathbf{f}}(\mathbf{x} +$

$\delta)$ with that to the target image $\hat{\mathbf{f}}(\mathbf{x}_{\text{tar}})$, e.g., via a GPT-based judge for caption similarity or keyword matching. The underlined δ highlights **universal** (one perturbation per target), while the underlined expectations over \mathbf{x} and $\hat{\mathbf{f}}$ highlight **transfer** (across arbitrary images and models).

Since victim MLLMs are typically **unknown and closed-source**, we follow Jia et al. (2025); Li et al. (2025b) and optimize on an ensemble of vision-language pretrained image encoders $\mathcal{F} = \{f_{\theta_1}, \dots, f_{\theta_t}\}$ to obtain transferable features. Given a small source image set $\mathcal{X} = \{\mathbf{x}_j\}_{j=1}^n$, we introduce learning **one** universal perturbation per target \mathbf{x}_{tar} by solving the following empirical objective:

Proposition 3.2 (Empirical Optimization for Universal Targeted Transfer). Given a small source image set $\mathcal{X} = \{\mathbf{x}_j\}_{j=1}^n$ and the encoder ensemble $\mathcal{F} = \{f_{\theta_i}\}_{i=1}^t$, we solve

$$\delta_s \in \arg \min_{\delta \in \mathcal{S}} \sum_{j=1}^n \sum_{i=1}^t \mathcal{L}_{\text{train}}(\mathbf{x}_j + \delta, \mathbf{x}_{\text{tar}}; f_{\theta_i}), \quad (2)$$

where f_{θ_i} extracts image features and $\mathcal{L}_{\text{train}}(\cdot)$ is a feature-space surrogate that aligns $\mathbf{x}_j + \delta$ with \mathbf{x}_{tar} under f_{θ_i} , e.g., cosine/MSE distance. Eq. (2) is a tractable surrogate of Def. 3.1, and we evaluate transfer to unseen images and unknown victim MLLMs $\hat{\mathbf{f}} \sim \hat{\mathcal{F}}$ using $\mathcal{L}_{\text{eval}}(\mathbf{x} + \delta_s, \mathbf{x}_{\text{tar}}; \hat{\mathbf{f}})$.

4. Methodology

Overview. Under the UTTAA formulation in Sec. 3, we aim to learn a *single* perturbation δ for a given target image \mathbf{x}_{tar} using surrogate models, and evaluate its transfer to *unseen* source images and *unknown* victim MLLMs. Our MCRMO-Attack is detailed in the following subsections. Sec. 4.1 proposes MCA to reduce optimization variance by aggregating supervisory signals across a multi-crop target set. Sec. 4.2 introduces TR to enhance informative supervision by routing alignable tokens while regularizing non-alignable ones. Sec. 4.3 learns a meta-initialization that enables scalable target adaptation. Finally, Sec. 4.4 summarizes the overall two-stage optimization of our MCRMO-Attack.

4.1. Stabilizing Target Supervision via Multi-Crop Aggregation (MCA)

Why sample-wise approaches become unstable in the universal Setting. Targeted transferable attacks are typically *sample-wise*, aligning token representations between a random source crop and a *single* random target crop at its original resolution (Jia et al., 2025; Li et al., 2025b). When extended to the UTTAA setting, this update strategy becomes significantly more challenging to optimize. For a given target image, a pool of source images is available, and at each optimization step a *triple-randomization* occurs: a source image is randomly sampled from the pool,

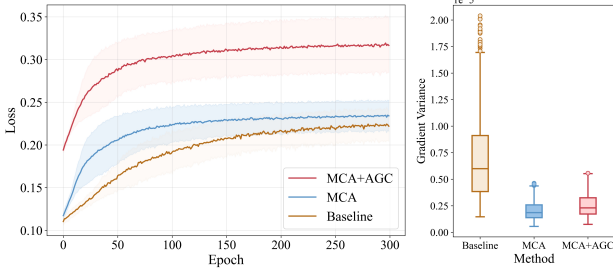


Figure 2. (Left) Comparison of mean loss curves with variance shading over 300 epochs, where the MCA and MCA+AGC variants exhibit improved convergence behavior relative to the baseline. (Right) Illustration of gradient variation, indicating that the proposed methods effectively reduce gradient stochasticity.

and both the source and target images undergo independent random cropping. As a result, the stepwise gradient is dominated by crop-specific local token variations, yielding a high-variance estimate of the intended objective. Consequently, the update may degenerate into a stochastic walk rather than progressing toward the expected optimum, leading to slow convergence and elevated gradient variance, as illustrated in yellow in Fig. 2.

To stabilize universal optimization, we propose **Multi-Crop Aggregation (MCA)**, which replaces “one target crop per step” with an aggregated estimate over a multi-crop target set. Intuitively, this enables the model to integrate information from multiple target crops, promoting robust learning of target-specific characteristics and alleviating the over-reliance on a single, potentially noisy crop. Prop. 4.1 further provides theoretical support for MCA by formalizing it as an unbiased Monte Carlo estimator with reduced variance. Moreover, we introduce an **Attention-Guided Crop (AGC)** as a persistent anchor, since regions with high attention contain richer semantic information, providing more informative signals that facilitate convergence to the optimum.

Proposition 4.1 (Monte Carlo Unbiasedness and Variance Reduction). *Let $v \sim p(v)$ denote a randomly sampled crop from the target image \mathbf{x}_{tar} at its original resolution, and define the per-crop objective as:*

$$\ell(\boldsymbol{\delta}; v) := \mathcal{L}(\boldsymbol{\delta}, v(\mathbf{x}_{\text{tar}})), \quad J(\boldsymbol{\delta}) := \mathbb{E}_{v \sim p(v)} [\ell(\boldsymbol{\delta}; v)]. \quad (3)$$

Given i.i.d. crops $\{v_i\}_{i=1}^m$ from $p(v)$, we consider the multi-crop estimator given below:

$$\widehat{J}_m(\boldsymbol{\delta}) := \frac{1}{m} \sum_{i=1}^m \ell(\boldsymbol{\delta}; v_i), \quad \widehat{g}_m(\boldsymbol{\delta}) := \nabla_{\boldsymbol{\delta}} \widehat{J}_m(\boldsymbol{\delta}). \quad (4)$$

Assume $\nabla_{\boldsymbol{\delta}} \ell(\boldsymbol{\delta}; v)$ is integrable and differentiation can be interchanged with expectation. Then, we have:

$$\begin{aligned} \mathbb{E}[\widehat{J}_m(\boldsymbol{\delta})] &= J(\boldsymbol{\delta}), \quad \mathbb{E}[\widehat{g}_m(\boldsymbol{\delta})] = \nabla_{\boldsymbol{\delta}} J(\boldsymbol{\delta}), \\ \text{Var}(\widehat{g}_m(\boldsymbol{\delta})) &= \frac{1}{m} \text{Var}(\nabla_{\boldsymbol{\delta}} \ell(\boldsymbol{\delta}; v)). \end{aligned} \quad (5)$$

Remark 4.2. Prop. 4.1 formalizes that replacing “one target crop per step” with a multi-crop target set yields an unbiased estimate of the distribution-level objective, while reducing gradient variance by a factor of $1/m$. This theoretical insight motivates MCA as a principled strategy to stabilize universal targeted optimization under limited steps.

Implementation. We instantiate MCA by representing the target with a small set of crops at the original resolution. Specifically, we first sample m crops $\mathcal{V}(\mathbf{x}_{\text{tar}}) = \{v_i(\mathbf{x}_{\text{tar}})\}_{i=1}^m$ at random. To provide a stable anchor signal, we add an attention-guided crop $v_{\text{attn}}(\mathbf{x}_{\text{tar}})$, which is centered on the peak activation of the surrogate model’s final-layer attention map and scaled to capture the most salient region. We denote the augmented crop set by:

$$\mathcal{V}^+(\mathbf{x}_{\text{tar}}) \triangleq \mathcal{V}(\mathbf{x}_{\text{tar}}) \cup \{v_{\text{attn}}(\mathbf{x}_{\text{tar}})\}. \quad (6)$$

For each target crop $v_{\text{tar}} \in \mathcal{V}^+(\mathbf{x}_{\text{tar}})$, we follow Jia et al. (2025) to extract token-level features and apply K-Means clustering to obtain a compact set of representative target embeddings, reducing redundancy while preserving discriminative semantics. Meanwhile, we extract token embeddings of the adversarial source crop $v_{\text{ps}} = v(\mathbf{x} + \boldsymbol{\delta})$. Formally, we define:

$$\{\mathbf{z}_{\text{tar}}^k\}_{k=1}^K = \text{KMeans}(f_{\theta}(v_{\text{tar}})), \quad \{\mathbf{z}_{\text{ps}}^l\}_{l=1}^L = f_{\theta}(v_{\text{ps}}), \quad (7)$$

where $\{\mathbf{z}_{\text{tar}}^k\}_{k=1}^K$ and $\{\mathbf{z}_{\text{ps}}^l\}_{l=1}^L$ denote the K target cluster centers and the L adversarial source features, respectively, and f_{θ} is the surrogate visual encoder. We then adopt the same alignment objective as Jia et al. (2025), applied independently to each target crop:

$$\mathcal{L}_{\text{MC}} = \sum_{k,l} \cos(\mathbf{z}_{\text{tar}}^k, \mathbf{z}_{\text{as}}^l) \cdot \pi_{kl}, \quad (8)$$

where π_{ts} is the optimal transport assignment weight, and we optimize by maximizing the multi-crop loss.

4.2. Token Routing (TR) via Alignability Gating

In the universal targeted setting, enforcing token-wise alignment equally across all source patches is unreliable, since a single perturbation must generalize across diverse images and thus cannot preserve instance-specific cues; as a result, indiscriminate alignment tends to create spurious correspondences and noisy supervision.

Exploit what aligns, preserve the rest. To this end, we propose **Token Routing (TR)**, which recognizes that not all source tokens are equally informative for learning a universal perturbation. For a given adversarial source crop, only a subset of tokens exhibits structural or semantic compatibility with the target. By emphasizing these alignable tokens, TR provides stable and transferable supervision by explicitly guiding the model to focus on the most relevant features.

Meanwhile, the remaining tokens are constrained to stay close to their original source counterparts $v_{\text{os}} = v(\mathbf{x})$, preventing them from pulling δ toward trivial or noisy patterns.

Implementation. For each adversarial source feature \mathbf{z}_{as}^l , we quantify its alignability $r(\mathbf{z}_{\text{as}}^l)$ to the target by computing its maximum cosine similarity with the target cluster centers $\{\mathbf{z}_{\text{tar}}^k\}_{k=1}^K$. This alignability score is then converted into a soft gating weight:

$$r(\mathbf{z}_{\text{as}}^l) = \max_k \cos(\mathbf{z}_{\text{as}}^l, \mathbf{z}_{\text{tar}}^k), \quad w(\mathbf{z}_{\text{as}}^l) = \sigma\left(\frac{r(\mathbf{z}_{\text{as}}^l) - \gamma}{\alpha}\right) \in (0, 1), \quad (9)$$

where $\sigma(\cdot)$ is sigmoid function, γ sets its threshold, and α controls its sharpness. The resulting $w(\mathbf{z}_{\text{as}}^l)$ acts as a soft gate, selectively emphasizing tokens aligned with the target while suppressing misaligned ones. We then define the routed targeting objective based on Eq. (8):

$$\mathcal{L}_{\text{TR}} = \sum_{k,l} \left(w(\mathbf{z}_{\text{as}}^l) \cdot (\mathcal{L}_{\text{MC}} + \lambda_{\text{pre}}(1 - w(\mathbf{z}_{\text{as}}^l)) \cdot \cos(\mathbf{z}_{\text{as}}^l, \mathbf{z}_{\text{os}}^l)) \right), \quad (10)$$

where $\mathbf{z}_{\text{os}}^l = f_{\theta}(v_{\text{os}})$ denotes the features of the original source crop. The first term encourages alignment between the attended source tokens and the target, while the second term preserves the original source semantics for suppressed tokens. We also incorporate a coarse-grained global feature alignment loss \mathcal{L}_{coa} via cosine similarity and a dynamic ensemble weighting strategy from Jia et al. (2025). The overall objective we seek to maximize is defined as:

$$\mathcal{L} = \sum_{i=1}^t W_i \left(\mathcal{L}_{\text{TR}}^i + \lambda_{\text{coa}} \cdot \mathcal{L}_{\text{coa}}^i \right), \quad (11)$$

where $\mathcal{L}_{\text{TR}}^i$ and $\mathcal{L}_{\text{coa}}^i$ are the losses computed on the surrogate encoder f_{θ_i} , and W_i is its dynamically updated weight.

4.3. Meta-Initialization for Scalable Target Adaptation

UTTAA is inherently a *many-target* problem: as new targets arrive, the attacker must produce a *per-target* universal perturbation. In practice, each target typically comes with only a small support set of source images for adaptation (Zhao et al., 2020; Zhang et al., 2021; 2025a), *i.e.*, $N \leq 20$. This *few-source* regime makes per-target optimization highly sensitive to initialization: with limited supervision, training from a zero initialization δ_0 is prone to drifting toward target- or sample-specific shortcuts, which weakens transfer and degrades the attainable performance. Prior work has also shown that, under few-shot adaptation settings, a well-learned initialization can act as a transferable prior and substantially improve the final solution quality (Zhao et al., 2020; Xia et al., 2024a; Zhou et al., 2025a). Motivated by these works, we do not treat each target in isolation. Instead, we learn a *generalizable prior* from *many meta tasks*, so that the initialization already encodes update directions that consistently support targeted universal transfer

across diverse targets. We therefore propose a *target-as-task meta-initialization* that provides a transferable warm start and yields stronger per-target performance in practice. Specifically, we sample N sources for each target τ_b from $\mathcal{D}_s = \{\mathbf{x}_i\}_{i=1}^{|\mathcal{D}_s|}$ as below:

$$\begin{aligned} \mathcal{I}_{\tau_b} &\subseteq \{1, \dots, |\mathcal{D}_s|\}, \quad |\mathcal{I}_{\tau_b}| = N, \\ \mathcal{I}_{\tau_b} &\sim \text{Uniform} \left(\left\{ \mathcal{I} \subseteq \{1, \dots, |\mathcal{D}_s|\} : |\mathcal{I}| = N \right\} \right), \quad (12) \\ \mathcal{X}_{\tau_b} &\triangleq \{\mathbf{x}_i : i \in \mathcal{I}_{\tau_b}\} \in \mathbb{R}^{N \times H \times W \times C}. \end{aligned}$$

Target-as-Task Meta-initialization. We meta-learn an initialization δ_0 that is optimized for adaptation: after a small number of inner steps on a few-shot support set, it should yield a strong per-target perturbation. We treat each target $\mathbf{x}_{\text{tar}} \sim \mathcal{D}_{\text{tar}}$ as a task τ and learn δ_0 via a first-order Reptile update (Nichol et al., 2018). Crucially, the inner adaptation operator is *identical* to our test-time multi-crop targeting procedure (same crop construction and the same alignment loss), so meta-learning directly optimizes the post-adaptation objective that makes δ_0 an *update prior* that amortizes per-target optimization.

Meta Objective. For task τ , the multi-crop target optimization applies I steps of a constrained attacker update on a small support set $\mathcal{X}_{\tau} = \{\mathbf{x}_1, \dots, \mathbf{x}_n\}$. We denote this inner adaptation operator by

$$\delta_{\tau} = U_{\tau}^{(I)}(\delta_0), \quad (13)$$

where δ_0 is the shared zero-initialization and $U_{\tau}^{(I)}(\cdot)$ includes the multi-crop selection and any stochastic cropping. The meta goal is to learn δ_0 that yields strong *post-adaptation* performance under the per-target budget:

$$J(\delta_0) = \mathbb{E}_{\tau \sim p(\mathcal{D}_{\text{tar}})} \left[\mathcal{L}_{\tau} (U_{\tau}^{(I)}(\delta_0)) \right], \quad (14)$$

where $\mathcal{L}_{\tau}(\cdot)$ is defined to be consistent with \mathcal{L} in Eq. (11).

Reptile Meta-update. To optimize the expected post-adaptation objective in Eq. (14) without backpropagating through the I inner steps, we adopt the first-order Reptile update (Nichol et al., 2018). At each meta iteration, we sample a mini-batch of tasks $\{\tau_b\}_{b=1}^B$, run the inner adaptation in Eq. (13) to obtain the post-adapt perturbations $\{\delta_{\tau_b}\}$, and move the initialization toward their average:

$$\delta_0 \leftarrow \Pi_{\|\delta\|_{\infty} \leq \epsilon} (\delta_0 + \eta(\bar{\delta} - \delta_0)), \quad \bar{\delta} = \frac{1}{B} \sum_{b=1}^B \delta_{\tau_b}. \quad (15)$$

$\Pi_{\|\delta\|_{\infty} \leq \epsilon}(\cdot)$ denotes the projection (clamp) in terms of ℓ_{∞} -norm with budget ϵ . Intuitively, $(\bar{\delta} - \delta_0)$ aggregates task-specific adaptation directions, yielding a first-order surrogate for the post-adaptation risk in Eq. (14). In Appendix, Proposition ?? and Remark ?? clarify how the Reptile update in Eq. (15) serves as a first-order procedure for optimizing the expected post-adaptation objective in Eq. (14).

Algorithm 1 INNERUPDATE for MCRMO-Attack

```

function InnerUpdate( $\delta$ ,  $\tau_b$ ,  $\mathcal{X}$ ,  $M$ ,  $\alpha$ )
Require: clean sources  $\mathcal{X}$ , target image  $\tau_b$ 
Require: init perturbation  $\delta$ , steps  $M$ , step size  $\alpha$ 
 $\mathcal{V}^+ \leftarrow \mathcal{V}(\tau_b) \cup \{v_{\text{attn}}(\tau_b)\}$  via Eq. (6)
for  $m \leftarrow 1$  to  $M$  do
  for all  $(x, v) \in \mathcal{X} \times \mathcal{V}^+$  do
     $\mathcal{L} \leftarrow \mathcal{L}(x, \delta, v)$  via Eq. (11)
     $\delta \leftarrow \delta$  updated with  $\mathcal{L}, \alpha$  via Eq. (16)
  end for
end for
return  $\delta$ 
end function

```

Algorithm 2 Overall optimization of MCRMO-Attack

- 1: **Input:** source pool \mathcal{D}_s , target pool \mathcal{D}_{tar} , meta-init epochs E , meta-init task batchsize B , meta-init inner steps I , meta-init step size η , adaptation steps M , adaptation step size α .
- 2: **Output:** meta-init perturbations δ_0 and per-target perturbations $\{\delta_{\tau_b}\}_{\tau_b \in \mathcal{D}_{\text{tar}}}$.
- 3: **Init:** $\delta_0 \leftarrow \mathbf{0}$
 - # Stage-1: Meta-initialization via Reptile Training of δ_0
- 4: **for** $e = 1$ to E **do**
 - 5: Sample meta-init tasks $\mathcal{D}_{\text{tar}}^{\text{sub}} = \{\tau_b\}_{b=1}^B \subset \mathcal{D}_{\text{tar}}$
 - 6: **for** $b = 1$ to B **do**
 - 7: Sample \mathcal{X}_{τ_b} via Eq. (12)
 - 8: $\delta_{\tau_b} \leftarrow \text{INNERUPDATE}(\delta_0, \tau_b, \mathcal{X}_{\tau_b}, I, \eta)$
 - 9: **end for**
 - 10: Update meta initialization δ_0 via Eq. (15)
- 11: **end for**
 - # Stage-2: Meta-to-target Adaptation to Each Target
- 12: **for all** $\tau_b \in \mathcal{D}_{\text{tar}}$ **do**
 - 13: Sample $\hat{\mathcal{X}}_{\tau_b}$ via Eq. (12)
 - 14: $\delta_{\tau_b} \leftarrow \text{INNERUPDATE}(\delta_0, \tau_b, \hat{\mathcal{X}}_{\tau_b}, M, \alpha)$
- 15: **end for**
- 16: **Return** δ_0 and $\{\delta_{\tau_b}\}_{\tau_b \in \mathcal{D}_{\text{tar}}}$

4.4. Meta-to-Target Adaptation for MCRMO-Attack

As shown in Alg. 1, for each inner update, we update δ with a projected FGSM (Goodfellow et al., 2015) based on the proposed loss defined in Eq. (11):

$$\delta \leftarrow \Pi_{\|\delta\|_\infty \leq \epsilon} (\delta + \alpha \cdot \text{sign}(\nabla_\delta \mathcal{L})). \quad (16)$$

The overall optimization is summarized in Alg. 2, where:

Stage-1: Meta (Reptile) Training of δ_0 . At meta epoch e , we sample sub-target tasks $\mathcal{D}_{\text{tar}}^{\text{sub}} = \{\tau_b\}_{b=1}^B \subset \mathcal{D}_{\text{tar}}$. For each task τ_b , we construct a multi-crop target set $\mathcal{V}^+(\tau_b)$. Let δ_{τ_b} denote the inner-updated perturbation for τ_b , and we then update the initialization δ_0 via Eq. (15).

Stage-2: Meta-to-target Adaptation to Each Target. For each target image $\tau_b \in \mathcal{D}_{\text{tar}}$, we build $\mathcal{V}^+(\tau_b)$ (Eq. 6) and start from the learned initialization δ_0 . Running M inner steps with the same projected sign update yields the per-target universal perturbation δ_{τ_b} , aiming to generalize across unseen samples and unknown closed-source MLLMs.

5. Experiments

Datasets. We follow prior works (Dong et al., 2023; Li et al., 2025b; Jia et al., 2025) by selecting 100 target images from the MSCOCO validation set (Lin et al., 2014). For each target, we sample 20 optimization images for training and 30 disjoint unseen images for evaluation from the NIPS 2017 Adversarial Attacks and Defenses Competition dataset (K et al., 2017), ensuring no data leakage.

Implementation Settings. We follow the experimental protocol in (Jia et al., 2025) unless otherwise specified. Specifically, we optimize an ℓ_∞ -bounded perturbation with budget $\epsilon = \frac{16}{255}$, step size $\alpha = \frac{1}{255}$, and 300 iterations. For evaluation, the closed-source MLLMs are GPT-4o (Achiam et al., 2023), Gemini-2.0 (Team et al., 2023), and Claude-sonnet-4.5 (Anthropic, 2025). We set meta epoch $E = 125$, per epoch tasks $B = 16$, meta inner steps $I = 5$, and meta-init step size $\eta = 1/255$. We set the number of optimization sources $N = 20$, the number of target crops $m = 4$, $\lambda_{\text{pre}} = 0.05$, $\lambda_{\text{coa}} = 1$, $\alpha = 0.2$, and route margin $\gamma = 0$. Analysis for these hyperparameters are in Sec. 5.2 and 5.3.

Competitive Methods. We include 5 baselines: AnyAttack (Zhang et al., 2025b), M-Attack (Li et al., 2025b), and FOA-Attack (Jia et al., 2025) represent sample-wise targeted transferable attack methods. We also include UAP (Moosavi-Dezfooli et al., 2017) as a fair reference via our reimplementation, where we replace the optimization used in FOA-Attack with the objective for targeted universal adversarial perturbations (Hirano & Takemoto, 2020). Finally, UnivIntruder (Xu et al., 2025) is a targeted universal attack that uses text prompts as targets.

Evaluation Metrics. We follow Jia et al. (2025); Li et al. (2025b) to use an LLM-as-a-judge protocol: the same closed-source model captions the target and adversarial images, and GPTScore measures their semantic similarity. We report attack success rate (ASR) (similarity > 0.3) and average similarity (AvgSim). We also include prior keyword matching rates (KMR): $\text{KMR}_a/\text{KMR}_b/\text{KMR}_c$ denote matching at least 1/2/3 of three annotated keywords.

5.1. Comparisons results

Tab. 1 summarizes universal targeted transfer to GPT-4o, Gemini-2.0, and Claude under seen (optimization-sample) and unseen evaluations. On the seen samples (bottom block), our method already achieves strong targeted steering with only one perturbation per target, clearly outperforming universal baselines and approaching sample-wise methods. For instance, on GPT-4o, it attains 85.5% ASR (vs. 66.7% for UAP and 15.0% for UnivIntruder), closing the gap to FOA-Attack and significantly surpassing AnyAttack, with similar trends on Gemini-2.0. On Claude, our universal perturbation even exceeds all sample-wise competitors. On the more

Table 1. Results on closed-source MLLMs. **Top:** performance on unseen test samples that are never used in optimizing the perturbation, **Bottom:** performance on the optimization samples used to learn the perturbation for each target (*i.e.*, “seen” during optimization).

Method	GPT-4o					Gemini-2.0					Claude				
	KMR _a	KMR _b	KMR _c	ASR	AvgSim	KMR _a	KMR _b	KMR _c	ASR	AvgSim	KMR _a	KMR _b	KMR _c	ASR	AvgSim
<i>Performance on Unseen Test Samples</i>															
AnyAttack (Zhang et al., 2025b)	8.0	3.0	0.1	6.1	0.04	8.9	3.8	0.2	6.4	0.04	5.6	2.6	0.2	5.3	0.03
M-Attack (Li et al., 2025b)	4.6	2.1	0.1	3.4	0.02	5.0	2.3	0.2	3.0	0.02	4.3	1.8	0.1	2.6	0.02
FOA-Attack (Jia et al., 2025)	4.5	1.9	0.1	3.3	0.02	5.6	2.2	0.2	3.1	0.02	4.2	1.7	0.1	2.6	0.02
UAP (Moosavi-Dezfooli et al., 2017)	37.5	23.3	5.6	38.0	0.17	40.2	25.3	6.4	36.8	0.17	9.5	5.4	0.7	8.7	0.05
UnivIntruder (Xu et al., 2025)	14.1	7.4	1.3	17.9	0.05	18.6	11.3	2.2	21.1	0.05	9.4	5.1	0.8	10.9	0.03
Our MCRMO-Attack	52.0	34.5	9.9	61.7	0.27	52.6	34.8	9.9	56.7	0.25	14.5	8.7	2.2	15.9	0.07
<i>Performance on Seen Samples (Used for Optimization)</i>															
AnyAttack (Zhang et al., 2025b)	7.9	3.2	0.3	6.2	0.04	9.2	4.1	0.3	6.4	0.04	5.6	2.3	0.3	5.0	0.03
M-Attack (Li et al., 2025b)	81.7	59.5	18.6	91.2	0.53	74.1	52.9	14.2	80.3	0.44	15.0	8.5	1.2	14.5	0.08
FOA-Attack (Jia et al., 2025)	84.1	60.9	20.1	93.0	0.57	80.0	57.1	17.5	85.4	0.48	18.6	10.5	2.1	18.0	0.10
UAP (Moosavi-Dezfooli et al., 2017)	62.6	41.1	10.5	66.7	0.32	60.2	40.7	11.2	61.3	0.29	14.9	8.3	1.6	13.8	0.07
UnivIntruder (Xu et al., 2025)	22.9	12.8	2.4	15.0	0.07	27.3	16.5	3.2	15.0	0.07	13.4	7.3	1.1	9.2	0.05
Our MCRMO-Attack	73.5	50.5	14.0	85.5	0.39	72.7	51.4	11.3	75.5	0.36	17.8	11.4	2.9	25.0	0.13
Clean	AnyAttack	M-Attack	FOA-Attack	UnivIntruder	Ours	Target	AnyAttack	M-Attack	FOA-Attack	UnivIntruder	Ours				

Figure 3. Visualization of adversarial images and perturbations for unseen sample.

stringent unseen-sample setting (top block), the advantage is larger and consistent across models and metrics, demonstrating robust universality: GPT-4o reaches 61.7% ASR vs. 38.0% for UAP with higher KMR (*e.g.* KMR_a 52.0% vs. 37.5%), and Gemini-2.0 shows the same pattern (ASR 56.7% vs. 36.8%, KMR_a 52.6% vs. 40.2%). Gains persist on Claude as well.

5.2. Performance Analysis

Few-source Trade-off with N . Tab. 2 varies the number of optimization samples N for learning one target-specific universal perturbation. We observe a clear fit-generalize trade-off: on seen samples, ASR peaks at small N (*e.g.*, 2 or 5), while larger N slightly hurts fitting; on unseen samples, performance improves monotonically with N across all three closed-source models. This suggests that increasing N injects more diverse source gradients, reducing reliance on instance-specific shortcuts and yielding more source-invariant perturbations. Overall, our method attains strong performance with a small N and achieves clearly better generalization on unseen sources.

Table 2. Few-source optimization results for our MCRMO-Attack. We vary the number of seen optimization samples N used to learn a single target-specific universal perturbation.

n-source	GPT-4o		Gemini		Claude	
	ASR	AvgSim	ASR	AvgSim	ASR	AvgSim
<i>Performance on Unseen Test Samples</i>						
$N = 2$	9.0	0.05	9.0	0.04	2.3	0.02
$N = 5$	27.0	0.13	25.0	0.11	7.7	0.03
$N = 10$	42.3	0.17	40.0	0.17	12.8	0.06
$N = 20$	61.7	0.27	56.7	0.25	15.0	0.07
<i>Performance on Seen Samples (Used for Optimization)</i>						
$N = 2$	95.0	0.63	85.0	0.53	15.0	0.06
$N = 5$	98.0	0.57	90.0	0.47	28.0	0.13
$N = 10$	87.0	0.47	89.0	0.44	23.0	0.11
$N = 20$	85.5	0.39	75.5	0.36	25.0	0.13

Sample Visualization. Fig. 3 compares adversarial images and perturbations on unseen sources under the same bound. Our method best preserves natural appearance while reliably steering outputs toward the target, indicating stronger cross-sample generalization. AnyAttack produces template-like patterns that repeat across inputs, suggesting limited adaptability. Sample-wise methods (M-Attack, FOA-Attack) are

Table 3. Ablation of Multi-Crop Aggregation (MCA), Attention-Guided Crop (AGC) and Token Routing Universal Targeting (TR) in our universal targeted transferable attack.

Components			GPT-4o		Gemini		Claude	
MCA	AGC	TR	ASR	AvgSim	ASR	AvgSim	ASR	AvgSim
<i>Performance on Unseen Test Samples</i>								
✓			38.0	0.17	36.8	0.17	8.7	0.05
	✓		46.7	0.20	44.7	0.19	11.3	0.06
✓	✓		46.3	0.21	38.7	0.18	10.3	0.06
✓	✓	✓	51.0	0.22	48.0	0.21	11.7	0.07
✓	✓	✓	52.0	0.22	49.0	0.21	10.0	0.06
<i>Performance on Seen Samples (Used for Optimization)</i>								
✓			66.7	0.32	61.3	0.29	13.8	0.07
	✓		68.5	0.33	61.0	0.28	19.5	0.10
✓	✓		73.0	0.34	64.0	0.29	26.5	0.12
✓	✓	✓	78.0	0.40	68.5	0.33	25.0	0.11
✓	✓	✓	80.5	0.38	70.0	0.33	24.5	0.12

Table 4. Effect of the number of target crops m in multi-crop aggregation. We report the Attack Success Rate (ASR) and Average Similarity (AvgSim) with varying crop numbers.

m	GPT-4o		Gemini		Claude	
	ASR	AvgSim	ASR	AvgSim	ASR	AvgSim
<i>Performance on Unseen Test Samples</i>						
$m = 2$	42.0	0.19	39.3	0.17	9.0	0.05
$m = 4$	61.7	0.27	56.7	0.25	15.9	0.07
$m = 8$	64.7	0.28	60.3	0.26	14.3	0.07
$m = 16$	61.7	0.27	60.7	0.26	17.3	0.08
<i>Performance on Seen Samples (Used for Optimization)</i>						
$m = 2$	69.0	0.31	57.0	0.25	23.5	0.09
$m = 4$	85.5	0.39	75.5	0.36	25.0	0.13
$m = 8$	88.0	0.43	81.0	0.39	28.5	0.13
$m = 16$	84.0	0.41	80.5	0.38	31.0	0.15

tightly coupled to the source structure, so their perturbations lose transferable semantics once decoupled from the specific input. UnivIntruder is optimized for text-level universality and thus discards image-specific details, resulting in weaker image-targeted transfer. The perturbation maps further show our method yields the most structured, semantically generalizable patterns, consistent with stronger transfer.

5.3. Ablation Study

Tab. 3 shows that MCA, AGV, and TR provide complementary gains on both seen and unseen splits. From the universal baseline, each component alone improves ASR/AvgSim, with larger benefits on harder models (notably Claude). The largest boost comes from combining MCA+AGV, indicating that diverse crops plus a salient view yield stronger and more stable target supervision. Adding TR further improves transfer in most cases by filtering non-alignable token gradients and improving alignable learning, giving the best overall results.

Effect of Multi-Crop Aggregation. We ablate MCA and its crop number m in Tab. 4. Overall, increasing m strengthens targeted transfer on both seen and unseen samples, validating that MCA improves target-semantic alignment for

Table 5. Comparison of results with and without meta-initialization. The upper half uses our meta-initialized perturbation δ_0 as the starting point for Stage-2, while the lower half (w/o meta-init) starts from a zero initialization.

Stage-2 Epoch	GPT-4o		Gemini		Claude	
	ASR	AvgSim	ASR	AvgSim	ASR	AvgSim
<i>With Meta-Init: Unseen Test Samples</i>						
50	54.7	0.23	49.0	0.21	11.8	0.06
100	56.3	0.25	53.3	0.22	12.5	0.06
200	59.7	0.26	56.7	0.25	11.7	0.07
300	61.7	0.27	56.7	0.25	15.0	0.07
<i>With Meta-Init: Seen Samples (Used for Optimization)</i>						
50	77.5	0.36	70.0	0.31	24.0	0.12
100	83.0	0.39	72.5	0.33	24.5	0.12
200	87.0	0.40	76.5	0.36	22.0	0.11
300	85.5	0.39	75.5	0.36	25.0	0.13
<i>w/o Meta-Init: Unseen Test Samples</i>						
50	25.0	0.11	22.0	0.11	4.3	0.03
100	42.3	0.18	39.0	0.17	9.3	0.06
200	48.0	0.21	44.0	0.19	9.7	0.06
300	52.0	0.22	49.0	0.21	10.0	0.06
<i>w/o Meta-Init: Seen Samples (Used for Optimization)</i>						
50	45.5	0.23	40.5	0.19	16.0	0.08
100	68.0	0.31	58.5	0.26	24.0	0.11
200	77.5	0.35	69.0	0.31	24.0	0.13
300	80.5	0.38	70.0	0.33	24.5	0.12

universal optimization. We also observe diminishing returns (and occasional mild fluctuations) under a fixed compute budget when m becomes large, consistent with the Monte Carlo variance reduction perspective in Theorem 4.1.

Ablation on Meta-Initialization. Tab. 5 shows that our meta-initialization markedly speeds up Stage-2 adaptation and improves generalization. Starting from the meta-initialized δ_0 , only 50 epochs already achieves strong seen performance (e.g., ASR 77.5%/70.0%/24.0% on GPT-4o/Gemini/Claude), approaching the best baseline while using far fewer updates. More importantly, under the same small budget, it delivers substantially higher unseen performance (ASR 54.7%/49.0%/11.8%), clearly surpassing the w/o-meta counterpart and existing baselines. In contrast, removing meta-initialization yields a less favorable starting point for Stage-2 and consistently underperforms across all epoch budgets, especially in the low-epoch regime, leading to weaker cross-sample transfer.

6. Conclusion

This work makes the first systematic study of *universal targeted transferable* adversarial attacks on closed-source MLLMs. We propose MCRMO-ATTACK, a two-stage universal framework that learns a meta-initialized perturbation from few source samples for scalable target adaptation and then performs meta-to-target adaptation to produce target-specific universal perturbations. To improve stability and universality, MCRMO-ATTACK integrates Multi-Crop Aggregation with Attention-Guided Crop together with alignability-gated token routing to focus updates on alignable structures. Extensive experiments show strong targeted steering and robust transfer on commercial MLLMs.

References

Achiam, J., Adler, S., Agarwal, S., Ahmad, L., Akkaya, I., Aleman, F. L., Almeida, D., Altenschmidt, J., Altman, S., Anadkat, S., et al. Gpt-4 technical report. *arXiv preprint arXiv:2303.08774*, 2023.

Anthropic. Introducing claude sonnet 4.5, 2025. <https://www.anthropic.com/news/claude-sonnet-4-5> [Accessed: 2026-01-21].

Bai, J., Bai, S., Chu, Y., Cui, Z., Dang, K., Deng, X., Fan, Y., Ge, W., Han, Y., Huang, F., et al. Qwen technical report. *arXiv preprint arXiv:2309.16609*, 2023a.

Bai, J., Bai, S., Yang, S., Wang, S., Tan, S., Wang, P., Lin, J., Zhou, C., and Zhou, J. Qwen-vl: A frontier large vision-language model with versatile abilities. *arXiv preprint arXiv:2308.12966*, 1(2):3, 2023b.

Dong, Y., Liao, F., Pang, T., Su, H., Zhu, J., Hu, X., and Li, J. Boosting adversarial attacks with momentum. In *Proc. IEEE Int'l Conf. Computer Vision and Pattern Recognition*, 2018.

Dong, Y., Pang, T., Su, H., and Zhu, J. Evading defenses to transferable adversarial examples by translation-invariant attacks. In *Proc. IEEE Int'l Conf. Computer Vision and Pattern Recognition*, 2019.

Dong, Y., Chen, H., Chen, J., Fang, Z., Yang, X., Zhang, Y., Tian, Y., Su, H., and Zhu, J. How robust is google's bard to adversarial image attacks? *arXiv preprint arXiv:2309.11751*, 2023.

Ganeshan, A., BS, V., and Babu, R. V. Fda: Feature disruptive attack. In *Proc. IEEE Int'l Conf. Computer Vision*, 2019.

Goodfellow, I. J., Shlens, J., and Szegedy, C. Explaining and harnessing adversarial examples. In *Proc. Int'l Conf. Learning Representations*, 2015.

Guo, Q., Pang, S., Jia, X., Liu, Y., and Guo, Q. Efficient generation of targeted and transferable adversarial examples for vision-language models via diffusion models. *IEEE Trans. on Information Forensics and Security*, 2024.

Hirano, H. and Takemoto, K. Simple iterative method for generating targeted universal adversarial perturbations. *Algorithms*, 13(11):268, 2020.

Hu, K., Yu, W., Zhang, L., Robey, A., Zou, A., Xu, C., Hu, H., and Fredrikson, M. Transferable adversarial attacks on black-box vision-language models. *arXiv preprint arXiv:2505.01050*, 2025.

Huang, H., Erfani, S., Li, Y., Ma, X., and Bailey, J. X-transfer attacks: Towards super transferable adversarial attacks on clip. *arXiv preprint arXiv:2505.05528*, 2025.

Jia, X., Gao, S., Qin, S., Pang, T., Du, C., Huang, Y., Li, X., Li, Y., Li, B., and Liu, Y. Adversarial attacks against closed-source mllms via feature optimal alignment. *arXiv preprint arXiv:2505.21494*, 2025.

Jiang, C., Wang, Z., Dong, M., and Gui, J. Survey of adversarial robustness in multimodal large language models. *arXiv preprint arXiv:2503.13962*, 2025.

K, A., Hamner, B., and Goodfellow, I. Nips 2017: Defense against adversarial attack. <https://kaggle.com/competitions/nips-2017-defense-against-adversarial-attack>, 2017. Kaggle.

Kong, C., Luo, A., Bao, P., Yu, Y., Li, H., Zheng, Z., Wang, S., and Kot, A. C. Moe-ffd: Mixture of experts for generalized and parameter-efficient face forgery detection. *IEEE Transactions on Dependable and Secure Computing*, 2025.

Kuang, J., Shen, Y., Xie, J., Luo, H., Xu, Z., Li, R., Li, Y., Cheng, X., Lin, X., and Han, Y. Natural language understanding and inference with mllm in visual question answering: A survey. *ACM Computing Surveys*, 57(8): 1–36, 2025.

Kurakin, A., Goodfellow, I. J., and Bengio, S. Adversarial examples in the physical world. In *Artificial intelligence safety and security*, pp. 99–112. Chapman and Hall/CRC, 2018.

Li, B., Zhang, Y., Chen, L., Wang, J., Pu, F., Cahyono, J. A., Yang, J., Li, C., and Liu, Z. Otter: A multi-modal model with in-context instruction tuning. *IEEE Trans. on Pattern Analysis and Machine Intelligence*, 2025a.

Li, Z., Liu, D., Zhang, C., Wang, H., Xue, T., and Cai, W. Enhancing advanced visual reasoning ability of large language models. *arXiv preprint arXiv:2409.13980*, 2024.

Li, Z., Zhao, X., Wu, D.-D., Cui, J., and Shen, Z. A frustratingly simple yet highly effective attack baseline: Over 90% success rate against the strong black-box models of GPT-4.5/4o/o1. In *Proc. Annual Conf. Neural Information Processing Systems*, 2025b.

Li, Z., Kong, C., Yu, Y., Wu, Q., Jiang, X., Cheung, N.-M., Wen, B., Kot, A., and Jiang, X. Saver: Mitigating hallucinations in large vision-language models via style-aware visual early revision. In *Proceedings of the AAAI Conference on Artificial Intelligence*, 2026.

Liang, K., Dai, X., Li, Y., Wang, D., and Xiao, B. Improving transferable targeted attacks with feature tuning mixup. In *Proc. IEEE Int'l Conf. Computer Vision and Pattern Recognition*, 2025.

Lin, J., Song, C., He, K., Wang, L., and Hopcroft, J. E. Nesterov accelerated gradient and scale invariance for adversarial attacks. *arXiv preprint arXiv:1908.06281*, 2019.

Lin, T.-Y., Maire, M., Belongie, S., Hays, J., Perona, P., Ramanan, D., Dollár, P., and Zitnick, C. L. Microsoft coco: Common objects in context. In *Proc. IEEE European Conf. Computer Vision*, pp. 740–755, 2014.

Lin, X., Yu, Y., Yu, Z., Meng, R., Zhou, J., Liu, A., Liu, Y., Wang, S., Tang, W., Lei, Z., et al. Hidemia: Hidden wavelet mining for privacy-enhancing medical image analysis. In *Proceedings of the 32nd ACM International Conference on Multimedia*, 2024.

Lin, X., Liu, A., Yu, Z., Cai, R., Wang, S., Yu, Y., Wan, J., Lei, Z., Cao, X., and Kot, A. Reliable and balanced transfer learning for generalized multimodal face anti-spoofing. *IEEE Transactions on Pattern Analysis and Machine Intelligence*, 2025.

Liu, H., Li, C., Wu, Q., and Lee, Y. J. Visual instruction tuning. In *Proc. Annual Conf. Neural Information Processing Systems*, volume 36, pp. 34892–34916, 2023.

Lu, H., Liu, W., Zhang, B., Wang, B., Dong, K., Liu, B., Sun, J., Ren, T., Li, Z., Yang, H., et al. Deepseek-vl: towards real-world vision-language understanding. *arXiv preprint arXiv:2403.05525*, 2024.

Lu, H., Yu, Y., Yang, Y., Yi, C., Zhang, Q., Shen, B., Kot, A. C., and Jiang, X. When robots obey the patch: Universal transferable patch attacks on vision-language-action models. *arXiv preprint arXiv:2511.21192*, 2025.

Lu, H., Yu, Y., Xia, S., Yang, Y., Rajan, D., Ng, B. P., Kot, A., and Jiang, X. From pretrain to pain: Adversarial vulnerability of video foundation models without task knowledge. In *Proceedings of the AAAI Conference on Artificial Intelligence*, 2026.

Meng, R., Yi, C., Yu, Y., Yang, S., Shen, B., and Kot, A. C. Semantic deep hiding for robust unlearnable examples. *IEEE Transactions on Information Forensics and Security*, 2024.

Moosavi-Dezfooli, S.-M., Fawzi, A., Fawzi, O., and Frossard, P. Universal adversarial perturbations. In *Proc. IEEE Int'l Conf. Computer Vision and Pattern Recognition*, pp. 1765–1773, 2017.

Nichol, A., Achiam, J., and Schulman, J. On first-order meta-learning algorithms. *arXiv preprint arXiv:1803.02999*, 2018.

Salaberria, A., Azkune, G., de Lacalle, O. L., Soroa, A., and Agirre, E. Image captioning for effective use of language models in knowledge-based visual question answering. *Expert Systems with Applications*, 212:118669, 2023.

Team, G., Anil, R., Borgeaud, S., Alayrac, J.-B., Yu, J., Soricut, R., Schalkwyk, J., Dai, A. M., Hauth, A., Millican, K., et al. Gemini: a family of highly capable multimodal models. *arXiv preprint arXiv:2312.11805*, 2023.

Touvron, H., Lavril, T., Izacard, G., Martinet, X., Lachaux, M.-A., Lacroix, T., Rozière, B., Goyal, N., Hambro, E., Azhar, F., et al. Llama: Open and efficient foundation language models. *arXiv preprint arXiv:2302.13971*, 2023.

Wang, C., Yu, Y., Guo, L., and Wen, B. Benchmarking adversarial robustness of image shadow removal with shadow-adaptive attacks. In *IEEE International Conference on Acoustics, Speech and Signal Processing*, 2024a.

Wang, K., He, X., Wang, W., and Wang, X. Boosting Adversarial Transferability by Block Shuffle and Rotation. In *Proc. IEEE Int'l Conf. Computer Vision and Pattern Recognition*, 2024b.

Wang, X., He, X., Wang, J., and He, K. Admix: Enhancing the transferability of adversarial attacks. In *Proc. IEEE Int'l Conf. Computer Vision*, 2021a.

Wang, Z., Guo, H., Zhang, Z., Liu, W., Qin, Z., and Ren, K. Feature importance-aware transferable adversarial attacks. In *Proc. IEEE Int'l Conf. Computer Vision*, 2021b.

Wu, Q., Yu, Y., Kong, C., Liu, Z., Wan, J., Li, H., Kot, A. C., and Chan, A. B. Temporal unlearnable examples: Preventing personal video data from unauthorized exploitation by object tracking. In *Proceedings of the IEEE/CVF International Conference on Computer Vision*, 2025.

Xia, S., Yang, W., Yu, Y., Lin, X., Ding, H., Duan, L., and Jiang, X. Transferable adversarial attacks on sam and its downstream models. In *Proc. Annual Conf. Neural Information Processing Systems*, volume 37, pp. 87545–87568, 2024a.

Xia, S., Yu, Y., Jiang, X., and Ding, H. Mitigating the curse of dimensionality for certified robustness via dual randomized smoothing. In *International Conference on Learning Representations*, 2024b.

Xia, S., Yu, Y., Yang, W., Ding, M., Chen, Z., Duan, L.-Y., Kot, A. C., and Jiang, X. Theoretical insights in model inversion robustness and conditional entropy maximization for collaborative inference systems. In *Proceedings of the Computer Vision and Pattern Recognition Conference*, 2025.

Xie, C., Zhang, Z., Zhou, Y., Bai, S., Wang, J., Ren, Z., and Yuille, A. L. Improving transferability of adversarial examples with input diversity. In *Proc. IEEE Int'l Conf. Computer Vision and Pattern Recognition*, 2019.

Xu, B., Dai, X., Tang, D., and Zhang, K. One surrogate to fool them all: Universal, transferable, and targeted adversarial attacks with clip. In *Proceedings of the 2025 ACM SIGSAC Conference on Computer and Communications Security*, pp. 3087–3101, 2025.

Yang, F., Huang, Y., Wang, K., Shi, L., Pu, G., Liu, Y., and Wang, H. Efficient and effective universal adversarial attack against vision-language pre-training models. *arXiv preprint arXiv:2410.11639*, 2024.

Yu, Y., Yang, W., Tan, Y.-P., and Kot, A. C. Towards robust rain removal against adversarial attacks: A comprehensive benchmark analysis and beyond. In *Proceedings of the IEEE/CVF Conference on Computer Vision and Pattern Recognition*, 2022.

Yu, Y., Wang, Y., Yang, W., Lu, S., Tan, Y.-P., and Kot, A. C. Backdoor attacks against deep image compression via adaptive frequency trigger. In *Proceedings of the IEEE/CVF Conference on Computer Vision and Pattern Recognition*, 2023.

Yu, Y., Wang, Y., Xia, S., Yang, W., Lu, S., Tan, Y.-P., and Kot, A. Purify unlearnable examples via rate-constrained variational autoencoders. In *International Conference on Machine Learning*, 2024a.

Yu, Y., Zheng, Q., Yang, S., Yang, W., Liu, J., Lu, S., Tan, Y.-P., Lam, K.-Y., and Kot, A. Unlearnable examples detection via iterative filtering. In *International Conference on Artificial Neural Networks*, 2024b.

Yu, Y., Wang, Y., Yang, W., Guo, L., Lu, S., Duan, L.-Y., Tan, Y.-P., and Kot, A. C. Robust and transferable backdoor attacks against deep image compression with selective frequency prior. *IEEE Transactions on Pattern Analysis and Machine Intelligence*, 2025a.

Yu, Y., Xia, S., Lin, X., Kong, C., Yang, W., Lu, S., Tan, Y.-P., and Kot, A. C. Towards model resistant to transferable adversarial examples via trigger activation. *IEEE Transactions on Information Forensics and Security*, 2025b.

Yu, Y., Xia, S., Lin, X., Yang, W., Lu, S., Tan, Y.-P., and Kot, A. Backdoor attacks against no-reference image quality assessment models via a scalable trigger. In *Proceedings of the AAAI Conference on Artificial Intelligence*, 2025c.

Yu, Y., Xia, S., YANG, S., Kong, C., Yang, W., Lu, S., Tan, Y.-P., and Kot, A. Mtl-ue: Learning to learn nothing for multi-task learning. In *International Conference on Machine Learning*, 2025d.

Yu, Y., Zhang, Q., Ye, S., Lin, X., Wei, Q., Wang, K., Yang, W., Tao, D., and Jiang, X. Time is all it takes: Spike-retiming attacks on event-driven spiking neural networks. In *International Conference on Learning Representations*, 2026.

Zhang, C., Benz, P., Karjauv, A., and Kweon, I. S. Data-free universal adversarial perturbation and black-box attack. In *Proc. IEEE Int'l Conf. Computer Vision*, pp. 7868–7877, 2021.

Zhang, H., Wang, Y., Yan, S., Zhu, C., Zhou, Z., Hou, L., Hu, S., Li, M., Zhang, Y., and Zhang, L. Y. Test-time backdoor detection for object detection models. In *Proceedings of the IEEE/CVF Conference on Computer Vision and Pattern Recognition (CVPR)*, pp. 24377–24386, June 2025a.

Zhang, J., Wu, W., Huang, J.-t., Huang, Y., Wang, W., Su, Y., and Lyu, M. R. Improving adversarial transferability via neuron attribution-based attacks. In *Proc. IEEE Int'l Conf. Computer Vision and Pattern Recognition*, 2022a.

Zhang, J., Ye, J., Ma, X., Li, Y., Yang, Y., Chen, Y., Sang, J., and Yeung, D.-Y. Anyattack: Towards large-scale self-supervised adversarial attacks on vision-language models. In *Proc. IEEE Int'l Conf. Computer Vision and Pattern Recognition*, 2025b.

Zhang, P.-F., Huang, Z., and Bai, G. Universal adversarial perturbations for vision-language pre-trained models. In *Proceedings of the 47th International ACM SIGIR Conference on Research and Development in Information Retrieval*, pp. 862–871, 2024.

Zhang, Y., Tan, Y.-a., Chen, T., Liu, X., Zhang, Q., and Li, Y. Enhancing the transferability of adversarial examples with random patch. In *International Joint Conference on Artificial Intelligence*, 2022b.

Zhao, P., Ram, P., Lu, S., Yao, Y., Bouneffouf, D., Lin, X., and Liu, S. Learning to generate image source-agnostic universal adversarial perturbations. *arXiv preprint arXiv:2009.13714*, 2020.

Zhao, Y., Pang, T., Du, C., Yang, X., Li, C., Cheung, N.-M. M., and Lin, M. On evaluating adversarial robustness of large vision-language models. In *Proc. Annual Conf. Neural Information Processing Systems*, volume 36, pp. 54111–54138, 2023.

Zheng, Q., Yu, Y., Yang, S., Liu, J., Lam, K.-Y., and Kot, A. Towards physical world backdoor attacks against skeleton action recognition. In *European Conference on Computer Vision*, 2024.

Zhou, Z., Hu, S., Li, M., Zhang, H., Zhang, Y., and Jin, H. Advclip: Downstream-agnostic adversarial examples in multimodal contrastive learning. In *ACM Trans. Multimedia*, pp. 6311–6320, 2023.

Zhou, Z., Deng, M., Song, Y., Zhang, H., Wan, W., Hu, S., Li, M., Zhang, L. Y., and Yao, D. Darkhash: A data-free backdoor attack against deep hashing. *IEEE Transactions on Information Forensics and Security*, 2025a.

Zhou, Z., Hu, Y., Song, Y., Li, Z., Hu, S., Zhang, L. Y., Yao, D., Zheng, L., and Jin, H. Vanish into thin air: Cross-prompt universal adversarial attacks for sam2. *arXiv preprint arXiv:2510.24195*, 2025b.

Zhu, D., Chen, J., Shen, X., Li, X., and Elhoseiny, M. Minigpt-4: Enhancing vision-language understanding with advanced large language models. *arXiv preprint arXiv:2304.10592*, 2023a.

Zhu, H., Ren, Y., Sui, X., Yang, L., and Jiang, W. Boosting adversarial transferability via gradient relevance attack. In *Proc. IEEE Int'l Conf. Computer Vision*, 2023b.